



## ACL Morsky: Semi-automatic Tool for Assessing the Risk of Developing an Anterior Cruciate Ligament Injury

Anna Ghidotti<sup>1</sup>, Andrea Cattaneo<sup>1</sup>, Andrea Vitali<sup>1</sup>, Daniele Regazzoni<sup>1</sup> and Caterina Rizzi<sup>1</sup>

<sup>1</sup>University of Bergamo, [anna.ghidotti@unibg.it](mailto:anna.ghidotti@unibg.it)

<sup>1</sup>University of Bergamo, [andrea.cattaneo@unibg.it](mailto:andrea.cattaneo@unibg.it)

<sup>1</sup>University of Bergamo, [andrea.vitali1@unibg.it](mailto:andrea.vitali1@unibg.it)

<sup>1</sup>University of Bergamo, [daniele.regazzoni@unibg.it](mailto:daniele.regazzoni@unibg.it)

<sup>1</sup>University of Bergamo, [caterina.rizzi@unibg.it](mailto:caterina.rizzi@unibg.it)

Corresponding author: Andrea Vitali, [andrea.vitali1@unibg.it](mailto:andrea.vitali1@unibg.it)

**Abstract.** Anterior Cruciate Ligament (ACL) is one of the most injured ligaments. Various researches have studied the relationship between ACL rupture and the bony morphology attempting to understand why ACL rupture occurs. The most investigated predisposing factors in the scientific literature are mainly related to the femoral intercondylar notch and the tibial plateau. The aim of the present research is to create a semi-automatic tool for assessing the risk of developing an ACL injury. A package, named ACL Morsky, has been created in 3D Slicer to follow the entire workflow. The process starts with the load of DICOM data. Three-dimensional models are reconstructed by means of segmentation. Then, five parameters, considered risk factors for the ligament rupture, are measured both in 2D images and on 3D models. A specific algorithm compares the measured values with the range in literature to evaluate the probability of developing an ACL injury. The physician is provided with a report for the patient and his/her risk factors. Knowing in advance the risk of rupture can help in reducing it with preventive plans.

**Keywords:** Knee Injury, Morphological Parameters, Ligament Risk Factors, 3D Slicer, Knee Risk Assessment

**DOI:** <https://doi.org/10.14733/cadaps.2023.736-748>

### 1 INTRODUCTION

Anterior cruciate ligament (ACL) is a key structure in the knee. It runs from the femur to the tibia and stabilizes the joint, resisting anterior tibial translation and rotational loads. However, it is one of the most frequently injured ligaments, due to its anatomical structure and function [14]. The incidence is about 8.1/10,000 in the USA, but it becomes higher in active population, since ACL is most injured during high impact or sporting activities. Furthermore, ACL injuries can be related to meniscal and articular cartilage damage, that in the worst cases lead to the onset and progression of osteoarthritis with consequent pain for the patient. For this reason, preventive plans, that try to understand the risk factors for developing ACL injuries, are crucial for reducing them [38].

Many researches have studied the possible risk factors associated with an ACL rupture. They include patient characteristics, such as age, body mass index or sex, anatomic and biomechanical risk factors, intrinsic risk factors, such as genetic and extrinsic risk factors [30].

In particular, anatomic variations within general population may predispose to ligament rupture. Various studies in the literature have evaluated ACL injury and its association with variations in bony anatomy around the knee. Understanding femoral and tibial bony anatomy promotes greater awareness regarding the predisposition for these injuries [35]. In particular, risk assessment tools can be developed to identify athletes who may benefit from ACL injury prevention programs focusing on quadriceps, hamstring, and core activation exercises [31].

Anatomic variations can be quantified using measurement tools. Currently, the gold standard for the evaluation of the indicators is imaging techniques, such as plain radiographs, Computed Tomography (CT) or Magnetic Resonance (MR) images [42]. Tyler et al. have employed MR images to identify morphological variations in the knee. They have highlighted the importance to recognize both normal anatomy and anatomical variants within the knee in order to avoid inappropriate diagnosis, over investigation or ineffective intervention [43].

Nowadays, modern 3D modeling technologies allow to reconstruct 3D models starting from DICOM data. 3D modeling of human districts is growing in popularity due to its potential and possibilities offered also by 3D printing [8] [10]. 3D models can provide an accurate and realistic virtual representation, whereas traditional 2D imaging techniques do not always allow to fully understand the morphology. It is the case when the anatomical district of interest is not completely visible in a single slice, due to the principles of imaging acquisition. Furthermore, the evaluation of 3D models can not take into consideration cross section or flexion angle, which affect 2D measurements [42]. Linear and angular measurements can be taken thanks to the widespread software applications, that even allow to draw curves on the model surface. In addition, new indicators can be investigated in the 3D space for a better understanding of the district.

In this context, the aim of the present research is twofold. The first is to identify the set of the most used risk factors for the assessment of developing ACL injury. The second is the creation of a semi-automatic tool for evaluating the previously described parameters, combining the use of DICOM images and three-dimensional models of the knee. For this reason, ACL Morsky (**Risky Morphology for ACL** injury) has been implemented as an extension of 3D Slicer, an open-source software for biomedical image analysis. It has been designed to be operated by individuals with limited knowledge of 3D modeling, guiding the users through a schematic workflow. The first step is the load of DICOM images into the database. Then, 3D models are created through a segmentation process. Measurements are performed both in 2D images and on 3D models. The solution makes available an algorithm to perform a morphological evaluation of the bony anatomy to assess the risk of ACL rupture. The assessment is possible through a comparison between the taken measurements and defined ranges derived from the literature. The last step is the generation of a report to support the physician's decision. All these steps have been embedded in the same environment. The interaction with the platform is as simple as possible, to be easily used by the medical staff.

The scientific background of algorithms for ACL injury identification and prevention is presented in section 2. In section 3, the risk factors for developing an ACL injury found in the literature are described. Then, the method for the development of the tool is explained in section 4. A clinical application of the developed package is reported in section 5. Finally, conclusion and future work avenues are designed.

## 2 SCIENTIFIC BACKGROUND

ACL injury is usually detected by a radiologist who visually inspects MR images. In this way, the physician is able to determine the level of the injury (i.e. complete, partial or not injured ACL). Recent scientific literature deals with the issue of semi-automated detection of ACL injury. Štajduhar et al. present a decision-support system that differentiates between normal and injured ACLs in a semi-automatic way. It aids in establishing the diagnosis and preventing human errors [40]. Key et

al. propose a new method to detect highly accurate automatic meniscal tear and ACL injuries, employing images in the three anatomical planes [24].

The imaging study by Padoia and colleagues deviates from the theme of diagnosis [11]. They develop an algorithm based on artificial intelligence to extract and compare differences in the tibial and the femoral bony morphology between normal ACL and ACL-injured knees. The results point out the potential of statistical shape-modeling for the detection of anatomic risk factors for ACL injury [31]. Statistical shape modeling provides a powerful tool for describing and analyzing human anatomy. It identifies the main mode of variation of a population of a given anatomical entity and can approximate the total variance of that population to a selected threshold [5].

Polamalu et al. employ three-dimensional statistical shape modeling to study the bony morphology associated with ACL injury. In their research work, they use three different CAD software applications: Mimics to create 3D surface models of femur and tibia, 3D Slicer for their alignment and Seg3D to create uniform bounding boxes [33]. Changing software and interfaces can be uncomfortable and increase the number of human errors: it could be more efficient to have all the necessary tool in the same environment.

In such a context, 3D Slicer is a free, open-source and multi-platform software package widely used for medical, biomedical, and related imaging research [25]. It is organized into modules, each of which has a specific function, such as to segment or to measure objects. There is also the possibility to customize this environment, by means of the creation of extensions, built on proven python-scriptable open-source libraries such as Visualization Toolkit and Insight Toolkit. Among the available extensions, there is SlicerMorph, which enables biologists to retrieve, visualize, measure and annotate 3D specimen data obtained both from volumetric scans (CTs and MRs) or surface scanners. It provides users with modules to upload 3D volumes, to annotate 3D curve and patch-based landmarks, generate landmark templates, conduct geometric morphometric analyses of 3D organismal form using both landmark-driven and landmark-free approaches [36]. Furthermore, Auto3dgm is an existing method that allows for comparative analysis of 3D digital models representing biological surfaces, even in the 3D Slicer environment.

However, these tools require a reference dataset or at least a target model for the comparison by means of a landmark set of points. The method proposed in this research work does not require a control group or a target model because the reference range is taken from the literature. Therefore, an important step has been analysing the scientific literature to identify the risk factors with their respective ranges as described in the following section.

### 3 RISK FACTORS FOR ACL INJURY

Many researchers have studied the relationship between ACL injury and the bony morphology attempting to understand why ACL rupture occurs [26]. The bony anatomical and morphological predisposing factors for ACL injury described in the scientific literature focus primarily on the femoral intercondylar notch and the tibial plateaus [4] [28]. The former is the concave region between medial and lateral condyles. The latter is the medial and lateral side of the upper part of the tibia. In particular, the present study considers five of the most investigated parameters, since other indicators are still under discussion in the literature. Specifically, they are: notch shape, Notch Width Index (NWI), beta angle, alpha angle and lateral tibial slope.

The femoral intercondylar notch is an anatomic site of interest as it houses the ACL. Intercondylar notches can be classified according to their shapes, as A-shaped (narrow apex), U-shaped (wide apex), or W-shaped (double-peaked notch) [45], as shown in Figure 1. According to some studies, patients with A-shaped notches have a 2.3 times greater risk of ACL injury compared with patients with U-shaped or W-shaped notches (Table 1).

NWI is defined as the ratio between the Notch Width (NW) and the femoral bicondylar width (BCW) [26] [39]. Table 2 shows the cut-off values to be considered at risk.

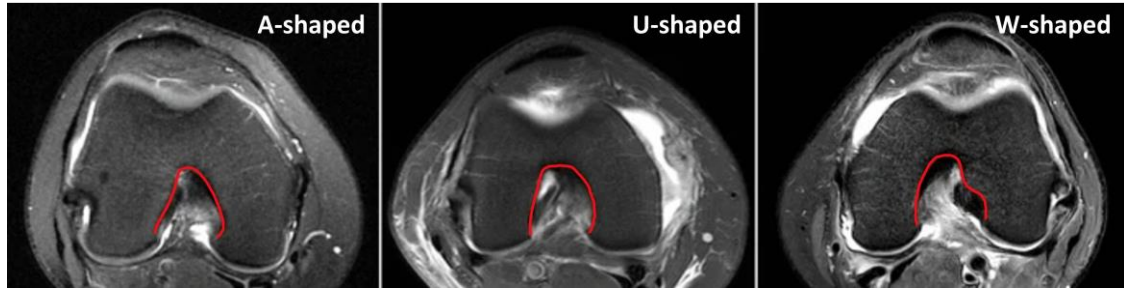


**Figure 1:** Different shapes of the femoral intercondylar notch [28].


A high angle between the femoral longitudinal axis and Blumensaat line, known as beta angle, has been thought to be a possible risk factor for ACL rupture as has the notch width angle (alpha angle) [26]. Table 3 and Table 4 report the cut-off risk values for beta and alpha angle, respectively.

Study	Risk shape
Al-Saeed et al. (2012) [2]	A-shape
Basukala et al. (2020) [7]	A-shape
Van Eck et al. (2010) [45]	A shape

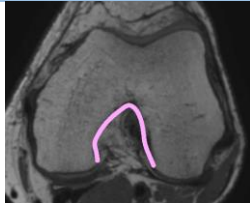


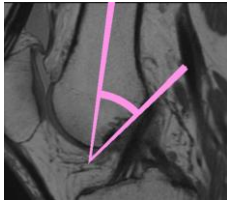
**Table 1:** Notch shape at risk for developing an ACL injury.

Study	Cut-off risk value
Al-Saeed et al. (2012) [2]	<0.269
Bouras et al. (2018) [9]	<0.270
Fahim et al. (2021) [15]	<0.290
Görmeli et al. (2014) [20]	<0.250
Hoteya et al. (2011) [22]	<0.250
Raja et al. (2019) [35]	<0.270
Shen et al. (2018) [37]	<0.252
Suprasanna et al. (2019) [41]	<0.263

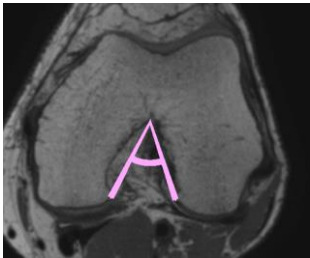


**Table 2:** Notch Width Index cut-off values for the risk of developing an ACL injury.

Study	Cut-off risk value
Jagodzinski et al. (2000) [23]	>37.7°
Shen et al. (2018) [37]	>38.5°

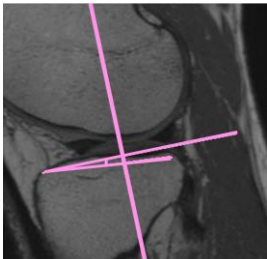
Wang et al. (2016) [46]	$>38.0^\circ$	
-------------------------	---------------	---

**Table 3:** Beta angle cut-off values for the risk of developing an ACL injury.

Study	Cut-off risk value	
Alentorn-Geli et al. (2015) [3]	$<50^\circ$	
Barnum et al. (2021) [6]	$<55^\circ$	
Gollwitzer et al. (2018) [19]	$<55^\circ$	
Lopes et al. (2017) [29]	$<60^\circ$	
Philippon et al. (2012) [32]	$<60^\circ$	

**Table 4:** Alpha angle cut-off values for the risk of developing an ACL injury.

Some studies have suggested that the morphology of the tibial plateau directly impacts the biomechanics of the joint [26]. The increased tibial slope is related to ACL injuries as it can cause a greater anterior displacement of the tibia [28]. In Table 5 some studies related to the lateral tibial slope with their cut-off values are reported.

Study	Cut-off risk value	
De Sousa Filho et al. (2021) [12]	$>8.00^\circ$	
Di Benedetto et al. (2020) [13]	$>8.70^\circ$	
Kumar Panigrahi et al. (2020) [27]	$>8.12^\circ$	
Shen et al. (2018) [37]	$>7.50^\circ$	
Ustabaşioğlu et al. (2020) [44]	$>8.51^\circ$	

**Table 5:** Lateral tibial slope cut-off risk values.

#### 4 METHOD AND TOOLS

A dedicated package for assessing the risk of developing an ACL lesion has been developed as an extension for 3D Slicer, to take advantage of the broad set of pre-processing tools available within this environment. This strategy has two advantages: (i) it allows users greater flexibility than an isolated software, and (ii) it allows for easier integration into manual/automated analysis pipelines for applications in the clinical environment.

The extension has been developed in Python, using the Qt framework for the user interface. It is based on a semi-automated work process. The user is guided through the entire workflow, from

the loading of DICOM data to the generation of a report of the morphological risk assessment. Five phases can be identified in this process, as shown in Figure 2. The first step is DICOM data load. The second phase is the segmentation, which permits the reconstruction of 3D models starting from the volume scan. In phase 3, the user is guided through the detection of the required key points on the bone surface. Subsequently, an automatic morphological evaluation is performed. The last step is the report generation which can be exported either in CSV or PDF file. Each step is described in the following subsections.

#### 4.1 Phase 1

The first step is the loading of DICOM data. Imaging equipment (CT and MR scanners) used in hospitals usually generates images saved as DICOM objects [1]. In the present case, MR images have been employed since they allow to recognize even the soft tissues.

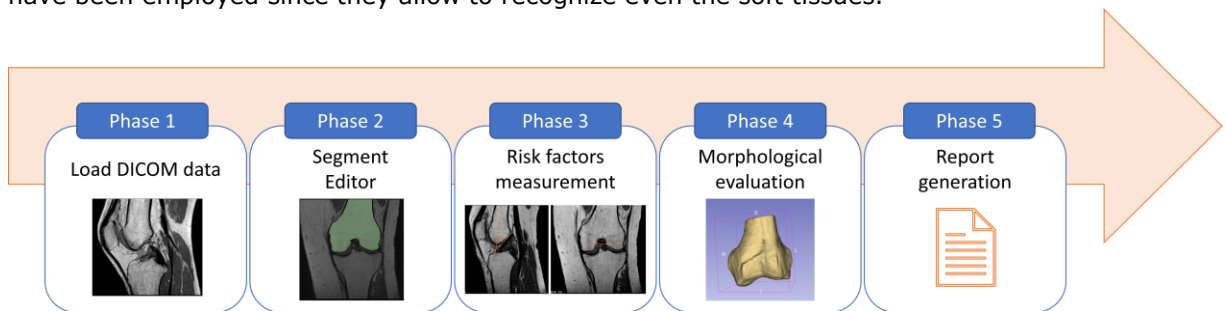


**Figure 2:** Workflow of the developed tool in 3D Slicer.

#### 4.2 Phase 2

The second phase is the image segmentation. Segmentation techniques can be divided, according to the user's involvement. The manual procedure requires the direct intervention of the user that draws or contours by hand the region of interest. The automatic approach involves an algorithm that identifies different regions with similar characteristics. A compromise between the previous two presented techniques is represented by the semiautomatic approach [17]. Different manual and semiautomatic tools are available in 3D Slicer, in 'Segment Editor' module [34]. In particular, bones can be reconstructed using 'Level tracing'. This algorithm consists in adding uniform intensity region to a segment, selected by the user. Then, some refinement can be done by means of manual tools. 'Draw' and 'Paint' allow to contour or paint the region of interest, to distinguish it from the background.

#### 4.3 Phase 3

In the third phase, the operator is asked to mark a number of key features over the tibial and femoral surface. Figure 3 shows the user interface of ACL Morsky. The user is guided step by step in the process of graphically state landmarks and reference lines for the definition of the five parameters to be measured. The main functionalities of the 3D Slicer module 'Markups' have been exploited for this purpose. It allows to measure positions, absolute distances, angles, volumes of the region of interest, open and closed curves. Reference points on the 3D models or in the images can be highlighted by means of landmarks. Both 2D and 3D modeling are employed for morphological assessment. Three of the five investigated risk factors are measured in 3D. In particular, they are related to the intercondylar notch, such as the notch shape, the alpha angle and the notch width index. The employment of 3D virtual models allows overcoming the issues associated with 2D images due to the principles of acquisition, such as the location of cross-section or flexion angles. They allow to appreciate all the region of interest, not only the part in the single slice. The other two angle parameters are measured in 2D. They imply the creation of the Blumensaat line for the beta angle

and the selection of the peak points for the tibial plateau, so a more natural 2D approach is employed.



**Figure 3:** Interface of ACL Morsky. Risk parameters are computed automatically from a small number of human-defined landmarks.

Absolute distances have been used to measure bicondylar and notch widths, which are necessary for the computation of the NWI. Angle markups have been employed for the measurement of alpha and beta angle, as well as the tibial slope. Curves can be used to highlight the intercondylar shape for the notch type recognition. They are even useful to contour regions of interest, computing their areas.

#### 4.4 Phase 4

The fourth step is the morphological evaluation, by means of an algorithm developed ad hoc. Computer-aided notch shape classification is beneficial to improve intra- and inter-rater reliability, as reported by Hirtler et al. [21]. For this reason, the intercondylar notch shape is evaluated automatically from the curve drawn by the operator. The algorithm is structured into two phases. First, the slope of the tangent to the notch curve is examined to determine if it is U-shaped. If it is not, the ratio of the distance between the sides at the bottom and the middle is checked. If it differs more than  $\pm 7.5\%$ , the notch is classified as A-shaped, otherwise U-shaped. Next, NWI, beta angle and alpha angle are computed from the user input, according to their definitions. Lastly, the tibial slope is computed as described by Ghosh et al. [18]. From the midpoints of the anterior to posterior (AP) distal and proximal tibial width the tibial axis is identified. Then, the tibial slope is evaluated in the sagittal plane passing through the midpoint of the lateral tibial plateau as the angle between the perpendicular to the tibial axis and the straight line connecting the two peak points of the tibial plateau.

To date, a definitive consensus has not been reached in the scientific literature on which values should be considered risky for the parameters under consideration. Therefore, in ACL Morsky, it has been decided to apply a conservative approach by choosing the most restrictive thresholds among those identified. The calculated parameters are evaluated through the thresholds of risk indicators available in the literature, reported in Tables 1-5 in section 3. The cut-off values are summarized in Figure 4. If the value is in the safe range, a 0 score is assigned. Otherwise, a 1 score is allocated. Hence, the sum of the scores is computed. The higher the score is, the higher the probability is to be at risk of developing an ACL injury.

#### 4.5 Phase 5

The results of the ACL risk assessment are presented on the user interface through a table. Moreover, the analysis can be exported in a report either as CSV or PDF file. The report includes the generalities of the patient, a summary of the risk of an ACL injury, and the values of each parameter evaluated by ACL Morsky. The patient's information is obtained directly from the DICOM files using the built-in 3D Slicer DICOM module. For the CSV generation, Python's *csv* built-in module is exploited. The PDF is generated using the *qSlicerWebWidget* class by means of a template written in HTML.

3D measurements			2D measurements		
Notch shape	NWI	Alpha angle	Beta angle	Tibial slope	
1 	A-shape	< 0.29	< 60°	> 37.70°	> 7.50°
0 	U/W shape	≥ 0.29	≥ 60°	≤ 37.70°	≤ 7.50°

**Figure 4:** Cut-off values for the computation of the risk, that have been measured on 3D models and in 2D images, respectively.

## 5 APPLICATION AND DISCUSSION

In this section, the phases have been explained in detail for a clinical case. To test the capability of the developed tool to assess the risk factors for ACL rupture, a patient with a confirmed diagnosis of ACL rupture has been involved. MR images of a patient have been loaded and bones have been reconstructed by means of manual and semi-automatic segmentation tools. Then, the user is guided during the measurement phase.

The notch shape type is identified, using the curve that follows the notch surface, as shown in Figure 5(a). In this case, an A shape is recognized. The bicondylar and notch widths have been measured as shown in Figure 5(b). Bicondylar width (BCW) has been measured starting from the popliteal groove of the lateral femoral condyle. On the same line, most interior margins of the femoral condyles are identified. The distance between these margins represents the NW. The NWI is calculated by dividing the NW by the BCW. The notch angle (alpha angle) is formed between the most inferior aspect of the notch at the medial and lateral condyles and the top of the intercondylar notch, as shown in Figure 5(c).

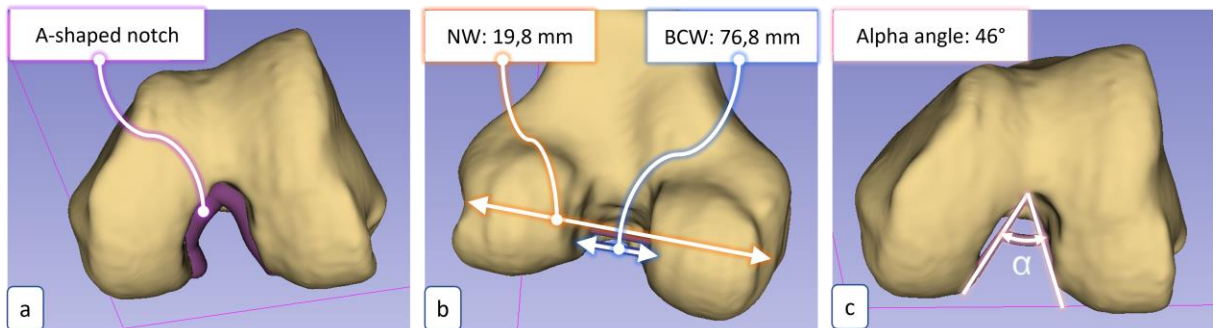


**Figure 5:** (a) A-shaped notch, (b) NW and BCW for the computation of NWI, (c) Alpha angle.

Beta angle has been measured in the sagittal plane. It is formed by the intersection between the sagittal longitudinal axis of the femur and Blumensaat line, as shown in Figure 6(a). To study the tibial plateau, the longitudinal axis of the tibia and the anterior and posterior peak points on the lateral tibial plateau are identified [16]. The lateral tibial slope (LTS) is measured relative to the axis perpendicular to the longitudinal axis and it is shown in Figure 6(b).



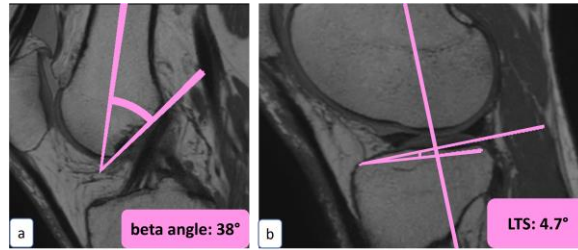


**Figure 6:** (a) Beta angle in the sagittal plane (b) Lateral tibial slope.

The developed algorithm automatically compares the performed measurements with the cut-off values. For the presented clinical case, four of the five parameters are out of the safe range. In this first prototype, each parameter has the same weight for the computation of the total risk. Thus, in the presented clinical case, the patient is assigned a score of 4 out of 5 for the risk of developing an ACL injury. However, a validation of the tool in a clinical trial will allow to identify the most significant parameters and their potential interdependencies. In future releases, different weights will be assigned to each parameter according to their influence on the risk. A report is generated and shown in Figure 7. It summarizes the patient's generalities, the measured values of the parameters and the respective probability risk. Finally, the total risk is computed.



**Figure 7:** PDF Report for the studied patient.

## 6 CONCLUSIONS

ACL Morsky is a 3D Slicer module developed for the assessment of the risk probability of developing an ACL injury. Since ACL rupture is frequent, especially in the active population, knowing the risk in advance is useful to take preventive actions. The application is intended to be used by physicians without specific technical modeling expertise, thus the interface has been designed to be as simple as possible. The software allows the operator to perform an assessment semi-automatically, reducing the subjectivity of the analysis. In this way, improved inter- and intra-rater reliability are expected; future studies are needed to confirm this claim. In addition, the integration of ACL Morsky into the open-source medical imaging software 3D Slicer enables the incorporation of the morphological evaluation into established clinical workflows. A clinical case has been presented to test its capability of computing the risk, taking into consideration five of the most investigated parameters in the literature. However, in the future additional morphologic parameters may be included to perform a broader analysis. In this light, recent studies are investigating the links between knee morphology and the likelihood of postoperative problems after cruciate ligament reconstruction [16]. Those relations could be exploited by future enhancements of the tool. Furthermore, since ACL Morsky is strongly anchored in the most established parameters in the literature, its analysis is tied to

measurements on two dimensions. The ability to model knees in 3D provides an opportunity to develop new and potentially more accurate indicators of ACL injury risk in the future.

Anna Ghidotti, <https://orcid.org/0000-0002-6415-3167>  
 Andrea Cattaneo, <https://orcid.org/0000-0002-6911-7042>  
 Andrea Vitali, <https://orcid.org/0000-0001-9261-4357>  
 Daniele Regazzoni, <https://orcid.org/0000-0001-5533-7047>  
 Caterina Rizzi, <https://orcid.org/0000-0002-1779-5183>

## REFERENCES

- [1] 3D Slicer, [https://slicer.readthedocs.io/en/latest/user\\_guide/modules/dicom.html](https://slicer.readthedocs.io/en/latest/user_guide/modules/dicom.html)
- [2] Al-Saeed O, Brown M, Athyal R, Sheikh M. Association of femoral intercondylar notch morphology, width index and the risk of anterior cruciate ligament injury, *Knee Surg Sports Traumatol Arthrosc*, 21(3), 2013, 678-82. <https://doi.org/10.1007/s00167-012-2038-y>
- [3] Alentorn-Geli, E.; Pelfort, X.; Mingo, F.; Lizano-Díez, X.; Leal-Blanquet, J.; Torres-Claramunt, R.; Hinarejos, P.; Puig-Verdié, L.; Monllau, J.C.: An Evaluation of the Association Between Radiographic Intercondylar Notch Narrowing and Anterior Cruciate Ligament Injury in Men: The Notch Angle Is a Better Parameter Than Notch Width, *Arthroscopy*, 31(10), 2015, 2004-13. <https://doi.org/10.1016/j.arthro.2015.04.088>
- [4] Andrade, R.; Vasta, S.; Sevivas, N.; Pereira, R.; Leal, A.; Papalia, R.; Pereira, H.; Espregueira-Mendes, J.: Notch morphology is a risk factor for ACL injury: a systematic review and meta-analysis, *Journal of ISAKOS*, 1(2), 2016, 70-81. <https://doi.org/10.1136/jisakos-2015-000030>
- [5] Audenaert, E. A.; Pattyn, C.; Steenackers, G.; De Roeck, J.; Vandermeulen, D.; Claes, P.: Statistical Shape Modeling of Skeletal Anatomy for Sex Discrimination: Their Training Size, Sexual Dimorphism, and Asymmetry, *Frontiers in Bioengineering and Biotechnology*, 7, 2019, <http://doi.org/10.3389/fbioe.2019.00302>
- [6] Barnum, M.S.; Boyd, E.D.; Vacek, P.; Slauterbeck, J.R.; Beynon, B.D.: Association of Geometric Characteristics of Knee Anatomy (Alpha Angle and Intercondylar Notch Type) With Noncontact ACL Injury, *Am J Sports Med.*, 49(10), 2021, 2624-2630. <https://doi.org/10.1177/03635465211023750>
- [7] Basukala, B.; Joshi, A.; Pradhan, I.: The Effect of the Intercondylar Notch Shape and Notch Width Index on Anterior Cruciate Ligament Injuries, *Journal of Nepal Health Research Council*, 17(4), 2020, 532-536. <https://doi.org/10.33314/jnhrc.v17i4.1858>
- [8] Bertolini, M.; Rossoni, M.; Colombo, G. Operative Workflow from CT to 3D Printing of the Heart: Opportunities and Challenges. *Bioengineering* 8, 2021, 130. <https://doi.org/10.3390/bioengineering8100130>
- [9] Bouras, T. ; Fennema, P. ; Burke, S. et al.: Stenotic intercondylar notch type is correlated with anterior cruciate ligament injury in female patients using magnetic resonance imaging, *Knee Surg Sports Traumatol Arthrosc* 26, 2018, 1252–1257. <https://doi.org/10.1007/s00167-017-4625-4>
- [10] Colombo, G.; Rizzi, C.; Regazzoni, D.; Vitali, A.: 3D interactive environment for the design of medical devices, *International Journal on Interactive Design and Manufacturing*, 12(2), 2018, 699–715. <https://doi.org/10.1007/s12008-018-0458-8>
- [11] Corban, J.; Lorange, J.-P., Laverdiere, C. et al.: Artificial Intelligence in the Management of Anterior Cruciate Ligament Injuries, *Orthopaedic Journal of Sports Medicine*, 2021. <http://doi.org/10.1177/23259671211014206>
- [12] De Sousa Filho P.G.T. ; Marques, A.C.; Pereira, L.S.; Pigozzo, B.A.; Albuquerque, R.S.P.E.: Analysis of Posterior Tibial Slope as Risk Factor to Anterior Cruciate Ligament Tear. *Rev Bras Ortop (Sao Paulo)*, 56(1), 2021, 47-52. <https://doi.org/10.1055/s-0040-1712495>
- [13] Di Benedetto, P.; Buttironi, M.M.; Mancuso, F.; Beltrame, A.; Gisonni, R.; & Causero, A.: Anterior cruciate ligament reconstruction: the role of lateral posterior tibial slope as a potential

- risk factor for failure. *Acta bio-medica: Atenei Parmensis*, 91(14-S), 2020, e2020024. <https://doi.org/10.23750/abm.v91i14-S.10996>
- [14] Duthon, V.B.; Barea, C.; Abrassart, S. et al. Anatomy of the anterior cruciate ligament, *Knee Surg Sports Traumatol Arthrosc*, 14, 2006, 204–213. <http://doi.org/10.1007/s00167-005-0679-9>
- [15] Fahim, S.M.; Dhawan, T.; Jagadeesh, N.; Ashwathnarayan, Y.P.: The relationship of anterior cruciate ligament injuries with MRI based calculation of femoral notch width, notch width index, notch shape - A randomized control study, *J Clin Orthop Trauma.*, 17, 2021, 5-10. <https://doi.org/10.1016/j.jcot.2021.01.006>
- [16] Ficek, K.; Rajca, J.; Cholewiński, J.; Racut, A.; Gwiazdoń, P.; Przednowek, K.; Hajduk, G.: Analysis of intercondylar notch size and shape in patients with cyclops syndrome after anterior cruciate ligament reconstruction, *Journal of orthopaedic surgery and research*, 16(1), 2021, 554. <https://doi.org/10.1186/s13018-021-02706-w>
- [17] Ghidotti, A.; Vitali, A.; Regazzoni, D.; Rizzi, C.: An investigation of innovative 3D modelling procedures for patient-specific Total Knee Arthroplasty, *Computer-Aided Design & Applications*, 19(2), 2022, 306-319. <https://doi.org/10.14733/cadaps.2022.306-319>
- [18] Ghosh G.: Effects of posterior tibial slopes on noncontact anterior cruciate ligament injury, *Saudi J Sports Med*, 15, 2015, 214-9. <http://doi.org/10.4103/1319-6308.164275>
- [19] Gollwitzer, H.; Suren, C.; Strüwind, C.; Gottschling, H.; Schröder, M.; Gerdesmeyer, L.; Proding, P.M.; Burgkart, R.: The natural alpha angle of the femoral head-neck junction: a cross-sectional CT study in 1312 femurs, *Bone Joint J.* 100-B(5), 2018, 570-578. <https://doi.org/10.1302/0301-620X.100B5.BJJ-2017-0249.R3>
- [20] Görmeli, C.A.; Görmeli, G.; Öztürk, Y.B.; Özdemir, Z.; Kahraman, A.: The Effect of The Intercondylar Notch Width Index on Anterior Cruciate Ligament Injuries: A Study on Groups with Unilateral and Bilateral ACL Injury, *Orthopaedic Journal of Sports Medicine*, 2014. <https://doi.org/10.1177/2325967114S00204>
- [21] Hirtler, L.; Tschematschar, K.; Käinberger, F.; Röhrich, S.: Applicability of Semi-Quantitative Evaluation of the Intercondylar Notch, *Applied Sciences*, 11(13) 2021. <https://doi.org/10.3390/app11135921>
- [22] Hoteya, K.; Kato, Y.; Motojima, S.; Ingham, S.J.; Horaguchi, T.; Saito, A.; Tokuhashi, Y.: Association between intercondylar notch narrowing and bilateral anterior cruciate ligament injuries in athletes, *Arch Orthop Trauma Surg*, 131(3), 2011, 371-6. <https://doi.org/10.1007/s00402-010-1254-5>
- [23] Jagodzinski, M.; Richter, G.; Pässler, H.: Biomechanical analysis of knee hyperextension and of the impingement of the anterior cruciate ligament: a cinematographic MRI study with impact on tibial tunnel positioning in anterior cruciate ligament reconstruction, *Knee Surgery* 8, 2000, 11–19. <https://doi.org/10.1007/s001670050004>
- [24] Key, S.; Baygin, M.; Demir, S. et al.: Meniscal Tear and ACL Injury Detection Model Based on AlexNet and Iterative ReliefF, *J Digit Imaging*, 2022. <https://doi.org/10.1007/s10278-022-00581-3>
- [25] Kikinis, R.; Pieper, S. D.; & Vosburgh, K. G.: 3D Slicer: A Platform for Subject-Specific Image Analysis, Visualization, and Clinical Support. In *Intraoperative Imaging and Image-Guided Therapy*, Springer, New York, NY, 2014, 277–289. [https://doi.org/10.1007/978-1-4614-7657-3\\_19](https://doi.org/10.1007/978-1-4614-7657-3_19)
- [26] Kızılgöz, V.; Sivrioğlu, A.-K.; Ulusoy, G.-R.; Aydın, H.; Karayol, S.-S.; Menderes, U.: Analysis of the risk factors for anterior cruciate ligament injury: an investigation of structural tendencies, *Clinical Imaging*, 50, 2018, 20-30. <https://doi.org/10.1016/j.clinimag.2017.12.004>
- [27] Kumar Panigrahi, T.; Das, A.; Mohanty, T.; Samanta, S.; Kumar Mohapatra, S.: Study of relationship of posterior tibial slope in anterior cruciate ligament injury, *J Orthop.*, 21, 2020, 487-490. <https://doi.org/10.1016/j.jor.2020.08.032>

- [28] Liu, F.; Zhang, S.; Xiao, Y. et al.: Stenotic intercondylar notch is not a risk factor for posterior cruciate ligament rupture: a morphological analyses using magnetic resonance imaging, *Knee Surg Sports Traumatol Arthrosc*, 2022. <https://doi.org/10.1007/s00167-021-06724-3>
- [29] Lopes, O.V.; Tragnago, G.; Gatelli, C.; Costa, R.N.; de Freitas Spinelli, L.; Saggin, P.R.F.; Kuhn, A.: Assessment of the alpha angle and mobility of the hip in patients with noncontact anterior cruciate ligament injury, *Int Orthop.*, 41(8), 2017, 1601-1605. <https://doi.org/10.1007/s00264-017-3482-6>
- [30] Misir, A.; Sayer, G.; Uzun, E.; Guney, B.; Guney, A.: Individual and Combined Anatomic Risk Factors for the Development of an Anterior Cruciate Ligament Rupture in Men: A Multiple Factor Analysis Case-Control Study, *The American Journal of Sports Medicine*, 50(2), 2022, 433-440. <http://doi.org/10.1177/03635465211062594>
- [31] Pedita, V.; Lansdown, D.A.; Zaid, M. et al.: Three-dimensional MRI-based statistical shape model and application to a cohort of knees with acute ACL injury, *Osteoarthritis Cartilage*, 23(10), 2015, 1695–1703. <http://doi.org/10.1016/j.joca.2015.05.027>
- [32] Philippon, M.; Dewing, C.; Briggs, K.; Steadman, J.R.: Decreased femoral head-neck offset: a possible risk factor for ACL injury. *Knee Surg Sports Traumatol Arthrosc.*, 20(12), 2012, 2585-9. <https://doi.org/10.1007/s00167-012-1881-1>
- [33] Polamalu, S.K.; Musahl, V.; Debski, R.E.: Tibiofemoral bony morphology features associated with ACL injury and sex utilizing three-dimensional statistical shape modeling, *Journal of Orthopedic Research*, 40(1), 2022, 87-94. <https://doi.org/10.1002/jor.24952>
- [34] Pinter, C.; Lasso, A.; Fichtinger, G.: Polymorph segmentation representation for medical image computing, *Computer Methods and Programs in Biomedicine*. 171, 2019, 19-26. <https://doi.org/10.1016/j.cmpb.2019.02.011>
- [35] Raja, B.; Marathe, N.; Desai, J.; Dahapute, A.; Shah, S.; Chavan, A.: Evaluation of anatomic risk factors using magnetic resonance imaging in non-contact anterior cruciate ligament injury, *J Clin Orthop Trauma*, 10(4), 2019, 710-715. <http://doi.org/10.1016/j.jcot.2019.02.013>
- [36] Rolfe, S.; Pieper, S.; Porto, A.; Diamond, K.; Winchester, J.; Shan, S.; Kirveslahti, H.; Boyer, D.; Summers, A.; Maga A.M.: SlicerMorph: An open and extensible platform to retrieve, visualize and analyse 3D morphology, *Methods Ecol Evol.*, 12, 2021, 816–1825. <http://doi.org/10.1111/2041-210X.13669>
- [37] Shen, L.; Jin, Z.G.; Dong, Q.R.; & Li, L.B.: Anatomical risk factors of anterior cruciate ligament injury, *Chinese medical journal*, 131(24), 2018, 2960-2967. <https://doi.org/10.4103/0366-6999.24720>
- [38] Shen, X., Xiao, J., Yang, Y. et al. Multivariable analysis of anatomic risk factors for anterior cruciate ligament injury in active individuals, *Arch Orthop Trauma Surg* 139, 1277–1285 (2019). <https://doi.org/10.1007/s00402-019-03210-x>
- [39] Simon, R.A.; Everhart, J.S.; Nagaraja, H.N.; Chaudhari, A.M.: A case-control study of anterior cruciate ligament volume, tibial plateau slopes and intercondylar notch dimensions in ACL-injured knees, *J Biomech*, 43(9), 2010, 1702-1707. <http://doi.org/10.1016/j.jbiomech.2010.02.033>
- [40] Stajduhar, I., Mamula, M., Miletić, D., Ünal, G.: Semi-automated detection of anterior cruciate ligament injury from MRI, *Computer Methods and Programs in Biomedicine*, 140, 2017, 151-164, <https://doi.org/10.1016/j.cmpb.2016.12.006>
- [41] Suprasanna, K.; Chamala, T.; Kumar, A.: Comparison of anatomical risk factors for noncontact anterior cruciate ligament injury using magnetic resonance imaging, *Journal of Clinical Orthopaedics and Trauma* 10(1), 2019, 143-148. <https://doi.org/10.1016/j.jcot.2017.08.002>
- [42] Toritsuka, Y.; Yamada, Y.: A View of Predisposing Factors by Novel 3D Imaging Techniques for the PF Joint, 2021, 249-263. [https://doi.org/10.1007/978-3-030-84748-7\\_21](https://doi.org/10.1007/978-3-030-84748-7_21)
- [43] Tyler, P.; Datir, A.; Saifuddin, A.: Magnetic resonance imaging of anatomical variations in the knee, *Skeletal Radiology*, 39, 2010, 1175–1186. <https://doi.org/10.1007/s00256-010-0904-6>
- [44] Ustabaşoğlu, F.E.; Samancı, C.; Aliş, D.: Evaluation of Intercondylar Notch, Condylar Morphology and Tibial Slope on Magnetic Resonance Imaging and their Influence on Rupture

- of the Anterior Cruciate Ligament, Haydarpasa Numune Med J., 60(2), 2020, 116-122 <https://doi.org/10.14744/hnhj.2018.48344>
- [45] Van Eck, C.F.; Martins, C.A.Q.; Vyas, S.M. et al.: Femoral intercondylar notch shape and dimensions in ACL-injured patients, Knee Surg Sports Traumatol Arthrosc, 18, 2010, 1257-1262. <https://doi.org/10.1007/s00167-010-1135-z>
- [46] Wang, H.M.; Shultz, S.J.; Schmitz, R.J.: Association of Anterior Cruciate Ligament Width With Anterior Knee Laxity, J Athl Train, 51(6), 2016, 460-5. <https://doi.org/10.4085/1062-6050-51.7.07>